



The United Nations
University

GEOTHERMAL TRAINING PROGRAMME
Orkustofnun, Grensasvegur 9,
IS-108 Reykjavik, Iceland

Reports 1994
Number 9

GEOCHEMICAL EVOLUTION OF THE AHUACHAPÁN GEOTHERMAL FIELD, EL SALVADOR, C.A.

Francisco Ernesto Montalvo López

Comisión Ejecutiva Hidroeléctrica del Río Lempa (C.E.L.),
Centro de Investigaciones Geotérmicas (C.I.G.),
km 11 1/2 Carretera al Puerto La Libertad,
Santa Tecla, La Libertad,
EL SALVADOR C.A.

ABSTRACT

More than 2800 fluid samples have been collected during the 20 years history of production from the Ahuachapán reservoir. A systematic analysis of this data shows a trend of dilution for the majority of the production wells. Also observed is a decline in enthalpy, both measured and based on geothermometers. This trend of dilution and declining reservoir enthalpy characterizes wells in the northern and northeastern sectors of the present wellfield. In the south and southwest, however, stable conditions are observed and the Na-K-Ca geothermometer indicates unchanged temperature. This is interpreted as two sources of recharge to the wellfield. The colder and less saline fluid recharges the reservoir in the northern sector and is most likely taken from the saturated reservoir zone above. The hot and deep recharge, on the other hand, comes into the wellfield from south. A simple lumped parameter model study indicates that 10-20% of the total mass produced is taken from the colder recharge. The mineral state of the reservoir fluid shows a low scaling potential for most of the present wells.

1. INTRODUCTION

In order to increase the production of electrical energy in El Salvador, a program of geothermal studies started in 1965. The first well drilled was AH-1 in Ahuachapán in 1968 with successful production results that allowed the development of the geothermal field with additional drilling of 31 wells. The field is located in the northwestern part of the country, approximately 20 km from the Guatemala border, 40 km from the Pacific Ocean, and 120 km from San Salvador, the capital city.

The operation of the field started with the installation of a 30 MW_e unit in 1975 and the second one in 1976. The third unit of 35 MW_e started its operation in 1980, bringing the installed capacity to 95 MW_e. The reservoir pressure fell by 10 bars in the period from 1975 to 1983. The cause for the drop in pressure, was considered overproduction of the reservoir. So after 1983, the field has been more carefully exploited but maintaining in operation the three units although not to their full capacity (Campos, 1985). For this reason, and considering also the limited natural energy resources in the country, the Comisión Ejecutiva Hidroeléctrica del Río Lempa (C.E.L.), has developed a geothermal project in order to increase production from the field, with the drilling of new wells and defining a reinjection strategy that will maintain pressure and allow more effective recovery of the heat stored in the reservoir. A systematic monitoring program of chemicals and production started in 1975.

The following report is a part of the 1994 UNU Geothermal Training Programme (during April to October) at Orkustofnun - National Energy Authority, Reykjavik, Iceland. The review, actualization and evaluation of the chemical behaviour of the Ahuachapán reservoir during all the production history of the field are presented. Also a conceptual model is elaborated with the new data, acquired in the continuous monitoring programme. Furthermore, the mineral state of the reservoir fluid is evaluated, because some wells have developed scaling problems in the last years. One of the main objectives of the field stabilization programme is the actualization of the physical-chemical, thermodynamic and productive characteristics, in order to define strategy to utilize the geothermal resource in the best way possible. So a general overview of the chemical changes in the reservoir due to the massive 15 year long extraction of fluid, may be of help for the aim to increase the electrical power and steam production from Ahuachapán.

2. THE AHUACHAPÁN GEOTHERMAL SYSTEM

2.1 Geology and hydrothermal alteration

The Ahuachapán geothermal field is associated with the southern flank of the central Salvadorean graben, and located at the northwest sector of the Cerro Laguna Verde volcanic group. This group constitutes a complex extrusive structure developed during Quaternary times near the Pliocene tectonic block of Tacuba-Apaneca, the regional faults which have controlled first the sinking of the graben and subsequently the emanation of volcanic products (Cuéllar et al., 1981).

The geothermal reservoir in the Ahuachapán geothermal system, seems to be controlled by the regional tectonic evolution with a fresh fracturation infiltration zone. The meteoric waters pass through the geological formation and become progressive in thermal waters. Furthermore, they reach the surface with the massive formation of hydrothermal alteration and fumarolic zones, distributed around an area of 50 km² (see Figure 1). This shows evidence of a weak tectonic system (CFG, 1992). The regional and local structures are controlled by a system of faults and fractures oriented along three main directions, E-W, which is approximately the trend of the main graben. To the west the field is bound by a second system of faults which strike NE-SW. Finally, superficial hydrothermal activity is

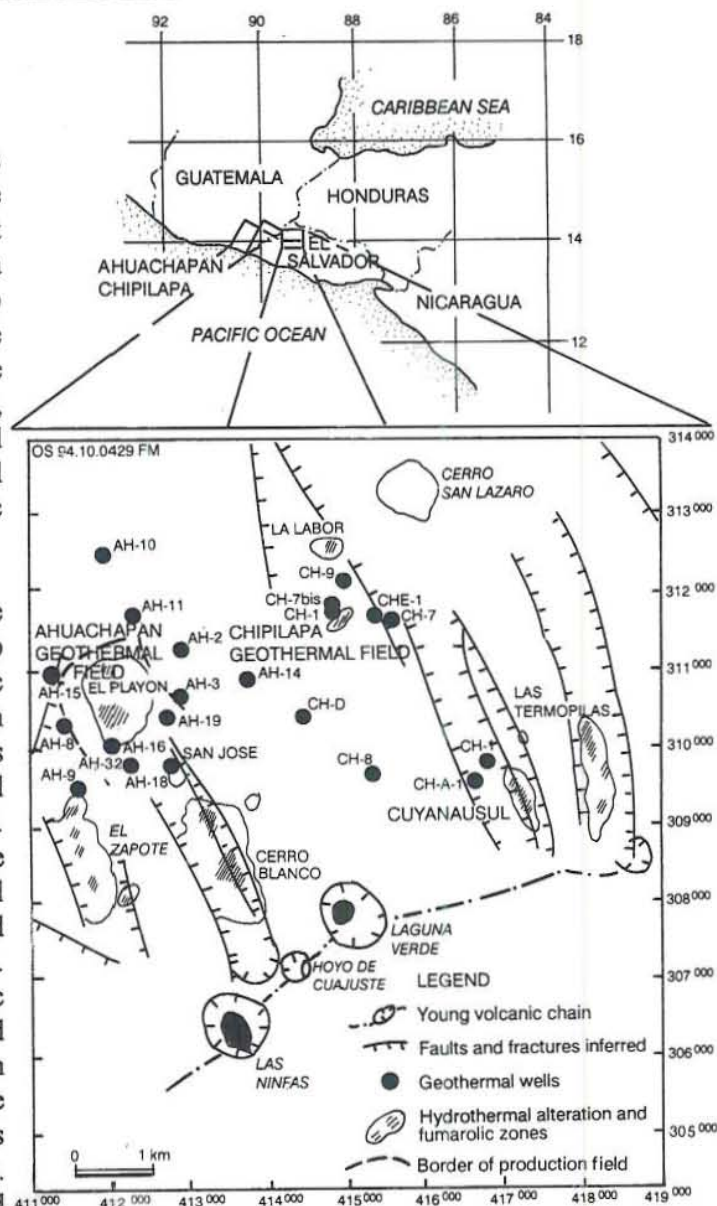


FIGURE 1: Main hydrothermal features and geological settings of the Ahuachapán and Chipilapa geothermal fields

associated with the most recent system of faults and fractures which have a NNW-SSE trend (Cuéllar et al., 1981). The stratigraphic sequence of the Ahuachapán area is mainly formed by, 1) tuff and lava formations (extrusive material) in the upper part of the system, with a thickness around 200 m; 2) young agglomerate formation that is essentially impermeable, due to a high hydrothermal alteration that forms the caprock of the reservoir with a thickness up to 400 m; 3) andesites of Ahuachapán, with a thickness up to 300 m that form the productive geothermal reservoir which has a typical secondary permeability; and 4) the older agglomerates in the lower part of the system, that form the basement with a thickness in excess of 400 m.

2.2 Geophysical exploration

The main results from the geophysical survey carried out in the area show a correlation between the geoelectric and gravimetric anomalies and the zones of hydrothermal activity. The most active ones are El Playón (near to the field) and Chipilapa-La Labor, close to the Chipilapa geothermal field (Figure 1). The border of the resistivity-low in the south part, corresponds to the old volcanic rocks which have higher resistivity than the adjacent Ahuachapán andesites in the geothermal field.

The present geophysical studies do not clarify if some continuity exists between the Ahuachapán reservoir and the Chipilapa field. However, the magneto-telluric and dipole-dipole results can be interpreted in such a way that a deep connection exists between these fields, until Cuyanausul-El Tortuguero fumarolic zone located in the eastern most extreme of the system. This hydrolic connection is hardly through the andsite formation since the Chipilapa wells intersected it without encountering permeable feedzones. Therefore, the lithological and petrological features of the geological formations and permeabilities in the Chipilapa and Ahuachapán wells are only partially related (Electroconsult, 1993). These arguments can only show an approach of the general boundaries of the system, but some detailed limits of the production reservoir are impossible to define, based on available data interpretation.

2.3 Hydrogeology and chemical features of the natural state

Three aquifers are defined within the Ahuachapán system, a) the shallow aquifer, b) the regional saturated aquifer, and c) the saline aquifer. This classification is based on the fluid chemistry temperature and the pressure response of the aquifers to seasonal rainfall variations, and each one corresponds with different lithologic units (Aunzo et al., 1991).

The groundwater zone within the shallow aquifer is found at 500 m a.s.l. This aquifer consists of tuff and pumices (extrusive material) covering the lavas of the Laguna Verde complex. This is a cool unconfined aquifer recharged by rainwater infiltration. It contains less than 500 ppm of total dissolved solids and is composed mainly of calcium carbonate type waters. The temperature in this aquifer ranges from 40 to 100°C with a decreasing trend toward north.

The regional saturated aquifer is found at the depth 300-500 m a.s.l. It consists of fractured lavas and pyroclastic deposits of tuff and lava formations (young agglomerates). Recharge takes place by direct infiltration which originates in shallow waters with a calcium-sodium carbonate composition below 400 ppm of TDS. An exception is a group of springs, of which the most important one is the El Salitre (70°C), with a mixture discharge characterized as sodium chloride type water. The spring is located about 7 km north of the Ahuachapán field and is related to the outflow of the geothermal system (Steingrímsson et al., 1991). The temperatures of this formation range from 110 to 130°C, decreasing toward north to El Salitre.

The saline aquifer is the geothermal reservoir of Ahuachapán. It is found below 300 m a.s.l. (500 m well depth), and consists of a sequence of andesitic lavas with extremely anisotropic and variable permeability. The salinity of the reservoir fluid prior to exploitation was up to 22,000 ppm of TDS (Romagnoli et al., 1976), and the measured fluid temperatures ranged from 214 to 240°C, with inferred minimum recharge

temperatures of 245-250°C, based on discharge fluid geothermometry (Aunzo et al., 1991). Initial data from Ahuachapán wells suggest that the source fluid is highly saline with chloride content up to 8000 ppm and up-flow temperatures above 250°C. The initial fluid chemistry in the Ahuachapán field indicated mixing in the reservoir between a more saline high temperature water and cooler less saline water (>130°C), which probably originated from the regional saturated aquifer that overlies the geothermal reservoir (Steingrímsson, et al., 1991) and is believed to come from the north and enter the reservoir from above or laterally. The chloride distribution suggests that the main inflow of the cooler water is in the eastern part of the production area (Truesdell et al., 1989). The natural state temperature (or liquid enthalpy) and chloride data were reasonably linear suggesting mixing of hot saline water with cooler, lower chloride waters (steam-heated?) at about 160°C, which may also correspond to waters of the regional saturated aquifer (Aunzo et al., 1991). With the production chemical data from 1985 at hand, and using early discharge data (before production), geothermometers (Na-K-Ca and SiO₂) and calculated aquifer chloride concentration showed a gradient from about 265°C and 9000 ppm Cl in the western part of the well field to 235°C and 6000 ppm Cl in the eastern part (Truesdell et al., 1989).

2.4 The Ahuachapán geothermal field

The 32 wells in Ahuachapán cover an area of around 4 km² and vary in depth between 591 and 1524 m. Their average elevation is about 800 m a.s.l. The first exploratory well drilled in Ahuachapán was well AH-1 in 1968. This well is located in the northern sector of the field. It turned out to be a very productive well and its success allowed for an intensive drilling programme to be carried out until 1981 when the last well AH-32 was drilled, in the southeastern part of the field.

The total installed capacity is 95 MW_e, but the present power output of the plant is around 64 MW_e (due to the pressure drawdown in the reservoir) using a total steam mass flow of 140 kg/s and 554 kg/s of water.

The location of the 95 MW_e power plant already constructed and the well field is shown in Figure 2.

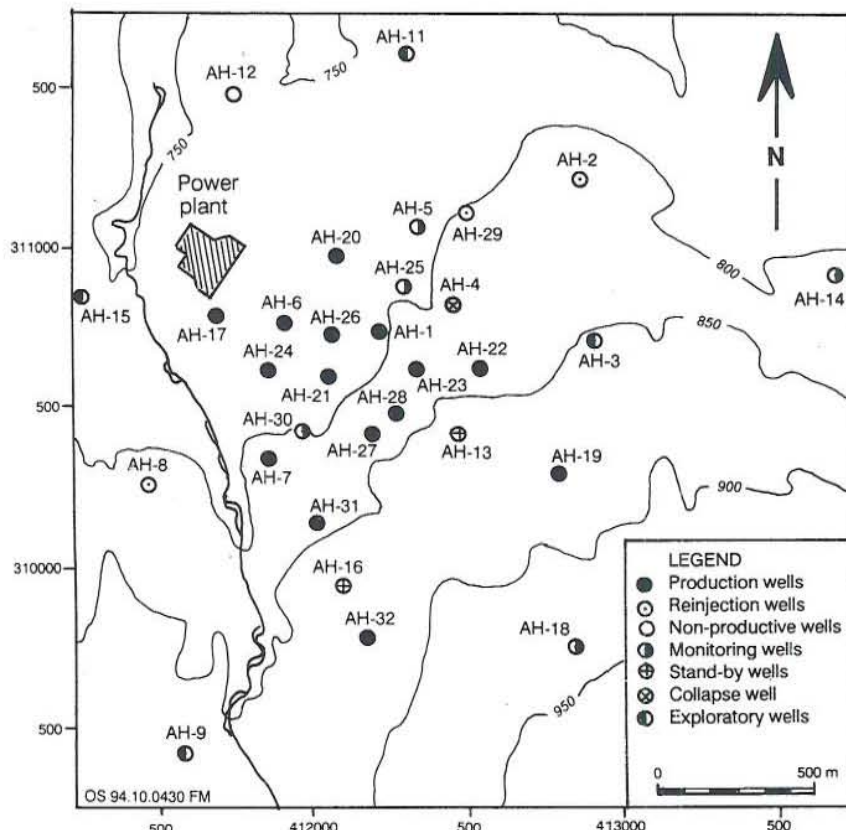


FIGURE 2: Location of the Ahuachapán geothermal field and the well distribution (modified from DiPippo, 1978)

At the present there are 15 production wells in an area of less than 2 km². Two of them, AH-17 and AH-32 have developed scaling problems in the last 3 years. The non-productive wells are used mainly for monitoring of reservoir temperature and pressure, and some wells are used for reinjection. A large-scale reinjection project was carried out from 1975, when the commercial exploitation of the field started, until 1982. Since then only minor experimental reinjection tests have been carried out.

The fluid extracted from the field is a two-phase mixture of steam and water, which is

conducted to wellhead separators to obtain medium-pressure steam, that directly feeds the three units of the power plant. The separated water phase is either separated again to get low-pressure steam for the third unit only (35 MW_e), reinjected or conducted to silencers and the residual water transported to the Pacific Ocean by a concrete channel (80 km long). The field is liquid-dominated, but it tends to be vapour-dominated in some of the production wells. The average temperature in the field is 210-220°C and the reservoir pressure (average) at 200 m a.s.l. is approximately 20 bar-a, compared to 37 bar-a initially. Almost all the wells exhibit separation pressure between 6-7 bar-a. The electrical power potential produced by the wells varies between 2.6 and 7.4 MW_e, and the total mass flow rate from 15 to 86 kg/s. General information on the production wells is listed in Table 1. It is possible to classify the production wells according to the measured enthalpy (average for the last two years), Table 2 shows this classification.

TABLE 1: General characteristics of the Ahuachapán production wells; earlier and actual aquifer temperature is a downhole average measured at the feedpoints; TP is two phase aquifer, L is liquid aquifer (data from LBL, 1988; and CEL, 1994)

Well no.	Year drilled	Depth (m)	Casing 9 ^{5/8} " OD (m)	Earlier & actual aquifer temp. (°C)	Main aquifer (m)	Steam fract. (%)	Power (MW _e)
AH-1	1968	1195	486.46	239-214	500 ^{TP} -550 ^L	10	3.3
AH-6	1970	591	454.3	232-209	480 ^{TP} -550 ^{TP}	78	4.4
AH-7	1970	950	483.36	226-220	520 ^{TP} -750 ^L	13	3.1
AH-17	1976	1200	450	225-205	468 ^{TP} , 870 ^L	100	6.1
AH-19	1978	1415	676	231-224	700 ^{TP} , 1100 ^L	14	3.5
AH-20	1974	850	450	220-205	460 ^{TP} -500 ^{TP}	20	5.8
AH-21	1975	849	500	227-210	500 ^{TP} -600 ^L	15	7.1
AH-22	1975	660	508.8	235-214	520 ^{TP} -600 ^L	34	2.6
AH-23	1977	924	459.5	224-215	460 ^{TP} -525 ^{TP}	22	4.5
AH-24	1976	850	411	223-209	452 ^{TP} -650 ^L	15	3
AH-26	1975	804	399	226-202	411 ^{TP} -650 ^L	43	2.8
AH-27	1978	800	412	236-219	425 ^{TP} -750 ^L	25	7.4
AH-28	1978	1000	428	227-224	450 ^{TP} -850 ^L	13	4.6
AH-31	1981	1502	489.8	232-225	560 ^{TP} -1000 ^L	14	6.1
AH-32	1985	1504	487.5	240-237	800 ^{TP} -1000 ^L	14	5.4

TABLE 2: A classification of production wells, based on fluid enthalpy; Hi is high enthalpy, Me is moderate or intermediate enthalpy, Lo is low enthalpy

Well no.	AH-17	AH-6	AH-26	AH-22	AH-23	AH-27	AH-20	AH-32
H (kJ/kg)	2785	2439	1594	1436	1294	1276	1094	1011
Type	Hi	Hi	Hi	Hi	Hi	Me	Me	Me
Well no.	AH-24	AH-21	AH-31	AH-7	AH-19	AH-28	AH-1	
H (kJ/kg)	1002	988	961	957	953	950	901	
Type	Me	Lo	Lo	Lo	Lo	Lo	Lo	

3. GEOCHEMICAL AND THERMODYNAMIC METHODOLOGY

3.1 The chemical data base and its statistical treatment

A long chemical history is available for Ahuachapán with data collected from the production wells at frequent intervals. Usually the water samples were taken monthly, but in some rare cases at least 4 times per year. Gas samples were also collected, generally duplicated, but not as frequently. A few downhole samples are available, mainly collected in the early period of exploitation. The number of samples available for the following study is around 2800 (counting both water and gas chemical results).

The fluid samples collected in Ahuachapán wells have been taken at the following locations:

- 1) Directly from weirboxes, next to the discharging wells; the majority of the available fluid samples are collected in this way according to the chemical data reports.
- 2) From water tanks which are used to regulate the separator pressure of each production well. This sampling procedure became necessary when the double flash unit 3 came on line and a large fraction of the separated fluid was piped directly to the power plant. Several samples collected after 1983 are taken in this way, however, specific information on which of the fluid samples are collected in the water tank are missing in the database used for this report. Only for the last 3 years have specific reports on the different sampling points been made.
- 3) The gas samples are either taken directly at the wellhead, the cyclonic separator or on the steam line, downstream from the individual separators.

The basis for the processing and interpretation of the data that have been used in the present work, was provided by the Analytical Chemistry Laboratory at the Geothermal Research Centre (CEL). The oldest data is from 1975-76, when systematic chemical monitoring of the field started. Also used are files processed by the Lawrence Berkeley Laboratory (LBL, 1988). Some difference was observed between LBL and the CEL data, mainly in the number of results used and the annual average calculated. For this reason the present data base, seems to be more complete and has been extended until July 1994.

In order to improve the accuracy of the chemical data history of each well, a statistical treatment using annual average was applied. Also, several plots of elements or chemical ratios against time were done. Both the plots and the statistical results were compared, allowing some data filtering, using the standard deviation and scattering coefficient. The data rejected this way seems to be not a part of the actual chemical history of some particular well, but rather due to incorrect sampling procedures or analysis. By using this methodology one may assume that only representative fluid samples of the wells are used for the following processing of Ahuachapán chemical history.

An Appendix to this study is published separately in a special report (Montalvo, F., 1994) showing the main data tables used and figures of chemical changes with time for all the wells. In this report, however, only wells AH-1 and AH-6 will be shown as representative of the reservoir, but other wells are also briefly included.

3.2 Conversion of surface fluid concentration to reservoir conditions

The large data base of chemical concentrations in Ahuachapán deals mostly with water samples that are collected at surface after separation of water and steam. It is of interest to convert these surface concentrations to the subsurface reservoir concentrations. This requires a set of simple formulas that are derived from the principles of mass and energy conservation. A major assumption for the derivation is that the dissolved solids are negligible in the separated steam phase and that non-condensable gases are negligible in the separated water phase.

The dissolved solid concentration in the reservoir is derived as follows. Assume we have a well discharging at a total flowrate m_t and an enthalpy h_t to a silencer. Assume furthermore that we measure the water flowrate m_{wb} and its chloride concentration Cl_{wb} in a weirbox. The principle of mass conservation for the chloride is then given as:

$$m_t Cl_{res} = m_{wb} Cl_{wb} = m_t (1 - x_a) Cl_{wb} \quad (1)$$

where Cl_{res} is the desired chloride concentration in the reservoir and x_a is the mass fraction of steam at atmospheric conditions. This mass fraction is derived from the well known energy balance

$$h_t = x_a h_{sa} + (1 - x_a) h_{la} \quad (2)$$

where h_{sa} and h_{la} are the steam and the water enthalpy at atmospheric pressure. Combining Equation 1 and 2 gives for the reservoir concentration

$$Cl_{res} = (1 - x_a) Cl_{wb} = \left[1 - \frac{h_t - h_{la}}{h_{sa} - h_{la}}\right] Cl_{wb} = \left[1 - \frac{h_t - 418}{2675 - 418}\right] Cl_{wb} \quad (3)$$

where 2675 and 418 are the steam and the water enthalpy in kJ/kg at atmospheric pressure.

Equations 1 and 2 also apply, slightly modified, if the fluid samples are taken from the water tanks, downstream from the Ahuachapán wellhead separators. The formulation requires that the water sample is cooled from the water tank temperature to room temperature, without any loss of steam. The water tank concentration, Cl_{sep} is then correlated with the reservoir concentration as:

$$Cl_{res} = (1 - x_{sep}) Cl_{sep} = \left[1 - \frac{h_t - h_{IPsep}}{h_{sPsep} - h_{IPsep}}\right] Cl_{sep} \quad (4)$$

Here P_{sep} is the separator pressure and h_l and h_s are water and steam enthalpies. Note that this equation is not valid if the water tank sample is allowed to boil down to atmospheric pressure and the steam discharged. For such cases, Equation 3 applies. Equations 3 and 4 apply directly for wells where flashing occurs inside the wellbore. Wells producing from two phase feedzones need special treatment (excess enthalpy wells).

Truesdell et al. (1989) suggest that instead of applying the wellhead enthalpy, h_t , in Equations 3 and 4, one should use the reservoir liquid enthalpy, h_{lres} . This is the liquid enthalpy which is assumed to reside at the single-phase, two-phase boundary next to the flowing well. This enthalpy may, for example be estimated by applying the Na-K-Ca geothermometer (Truesdell et al., 1989). The Na-K-Ca geothermometer depends on fractions between the Na, K and Ca concentrations. It is, therefore, only vaguely affected by the different mobilities of steam and the water phases in the reservoir, which on the other hand, may change the total concentration of these species. The wellhead enthalpy, h_p in Equation 3 and 4 is replaced by the Na-K-Ca reservoir enthalpy, h_{lres} , for the cases of high enthalpy wells in the Ahuachapán reservoir (see Chapter 3.4).

It may also be of interest to convert the water tank concentrations to weirbox concentrations. Setting up the mass conservation for chloride gives (using the same nomenclature as before)

$$m_{sep} Cl_{sep} = m_{wb} Cl_{wb} = (1 - x_a) m_{sep} Cl_{wb} \quad (5)$$

From the enthalpy balance we get for x_a

$$h_{lsep} = x_a h_{sa} + (1 - x_a) h_{la} \quad (6)$$

Rearranging terms for both Equations 5 and 6 finally gives the weirbox concentration:

$$Cl_{wb} = \frac{Cl_{sep}}{1 - x_a} = \frac{Cl_{sep}}{1 - \frac{h_{lsep} - h_{la}}{h_{sa} - h_{la}}} \quad (7)$$

The non-condensable gases are collected either at the wellhead or at the separator, most often at the separator pressure P_{sep} . In order to compare this data from one time to the other, the gas concentration is changed to atmospheric pressure. The procedure is as follows. Using the conservation of CO_2 mass we get:

$$m_{Ssep} CO_{2_{sep}} = m_{sa} CO_{2_a} \Leftrightarrow x_{sep} m_t CO_{2_{sep}} = x_a m_t CO_{2_a} \Leftrightarrow CO_{2_a} = \frac{x_{sep}}{x_a} CO_{2_{sep}} \quad (8)$$

Where m_{Ssep} and m_{sa} are the mass flow rates of steam at the separation and the atmospheric pressure respectively, and x_{sep} and x_a are the mass fraction of steam at separator and atmospheric pressures.

Finally, in order to find flow-weighted changes in the reservoir, the annual averages for the reservoir chloride and silica, measured enthalpy and Na-K-Ca enthalpy together with the annual flowrate average for each well were tabulated. Using the following formula with the chloride as an example, we find the annual field average:

$$\langle Cl_{fa} \rangle = \frac{m_1 \langle Cl_{res} \rangle_1 + \dots + m_n \langle Cl_{res} \rangle_n}{m_1 + \dots + m_n} \quad (9)$$

where $\langle Cl_{fa} \rangle$ is the reservoir chloride annual average for the field, using the monthly average of flow rate, m and the reservoir chloride content for all the individual wells. The result was plotted against time to observe the evolution of the main reservoir parameters.

3.3 Enthalpy-chloride mixing model

This mixing model takes into account both mixing and boiling processes, but the conductive cooling can also be illustrated. Its application basically involves the analysed chloride content and the water enthalpy, that can be obtained in different ways, such as from measured discharge temperatures, geothermometry, and silica-enthalpy mixing model temperatures (Arnorsson, 1985). For the utilization of this model in the report, measured discharge enthalpy values from the low-moderate enthalpy wells and the reservoir chlorine composition were plotted. The wells with high enthalpy discharge values use the Na-K-Ca geothermometer enthalpy and reservoir chlorine.

3.4 Enthalpy-geothermometry comparison

Deep fluid temperatures can be estimated using different geothermometers and the chemical analysis of produced fluids. When the thermodynamic conditions change in a reservoir, the kinetic rates of the chemicals involved in these geothermometers change in different way. That means the response time of the re-equilibrium conditions is different. If the fluid has a specific enthalpy higher than expected for liquid at the prevailing temperature, then comparison of geothermometer temperature may indicate reservoir processes, as the temperature of the fluid flowing into the well can change due to boiling, mixing with hotter or cooler fluids or if the fluid flows through hotter or colder rocks (Truesdell et al., 1989).

The Na-K-Ca geothermometer developed by Fournier and Truesdell (1973) requires a large amount of mineral transformation (exchange of K^+ ion for Na^+ and Ca^{++} on aluminosilicates) to change the fluid composition in a high or moderately saline fluid ($Cl > 2000$ ppm). So, the response at temperature changes for this geothermometer is slow. Therefore, it is assumed that the Na-K-Ca geotemperature represents the temperature of the fluid at a distance from the well and is not affected by mixing or boiling near the well. The quartz geothermometer is assumed to represent temperatures close to the well, and is usually fully equilibrated, which means the response to changes in temperature is quickly reached.

The enthalpy temperature is the temperature of liquid water calculated from the enthalpy of the total fluid produced by the well. The enthalpy temperature is the same as the actual inflow temperature, if the inflow is pure liquid phase. Boiling in the reservoir and two-phase flow towards wells lead to high enthalpy temperatures. The enthalpy temperature can be calculated from steam tables, using data for temperature and enthalpy for single-phase water. These two geothermometers and the enthalpy measured in wells can be applied in order to get indications of fluid state and temperatures near and far from the wells, and define the main process that is affecting a particular well. In the following work the enthalpy will be used to compare the Na-K-Ca and SiO_2 temperatures with the measured enthalpy. The temperature values were transformed to enthalpy using a simple polynomial and plotted with the annual average measured enthalpy for each well.

3.5 The distribution of chemical and thermodynamic properties

In order to illustrate the main changes observed in the production wells from the early exploitation period until 1993, several figures were drawn showing the areal distribution of the following parameters: reservoir chlorine (also the natural state from LBL is presented in the Appendix as a reference (Montalvo, 1994)), the quartz and Na-K-Ca temperature distribution, the measured discharge enthalpy and the gas-steam ratio (%w at separator pressure). The years 1978, 1985 and 1993 were chosen because most of the wells have complete chemical data for these years, but in this report only distributions for 1978 and 1993 are shown.

3.6 The WATCH programme and chemical data correction

The computer programme WATCH is a useful tool for the interpretation of the chemical composition of geothermal fluids, as well as for non-thermal waters. Some chemical analyses of samples collected at surface can be used to compute the composition of aquifer fluids. The programme involves the calculation of several aqueous species using mass balance equations and chemical equilibria. WATCH can also be used to calculate composition of the equilibrate sample after cooling or boiling (Arnorsson et al., 1982; Bjarnason, 1994).

For this purpose three main geothermal fluid models can be solved:

- 1) Two-phase inflow into well. The discharge is then also two-phase, so chemical data for both phases must be available.
- 2) Single-phase inflow into well. The discharge from the well can be either single-phase or two-phase. This model also can cover springs where the water has not boiled before collection.
- 3) Springs where the water has boiled and lost steam before the sample was collected.

When the first or the second model is selected, the input to the WATCH programme is taken from a file containing the results for each phase of analysis, including the water pH and the temperature at which it was measured. The water and the gas concentrations are required at the same conditions, which means the same sampling pressure. Another important input parameter is the reference temperature, i.e. the temperature at which the aqueous speciation is to be calculated. This reference temperature can be chosen as the measured temperature of the well (downhole), or as a geothermometer temperature value. The WATCH programme can

also be used to compute the resulting species concentrations, activity coefficients, activity products and solubility products when the equilibrated fluid is allowed to cool conductively or by adiabatic boiling from the reference temperature to some lower temperature. This is particularly useful in order to evaluate the scaling potential of the fluids. For the evaluation of the mineral state of the fluid, mainly for the quartz, calcite and anhydrite, several runs of WATCH programme were done for all the production wells, using the data results from 1990 to 1994, for water and gas samples. As most of this data was collected at different times and different sampling pressure conditions, it was necessary modify the data. This was done by using annual averages in order to get both results in the same conditions. For this purpose the equations in Chapter 3.2 were used to change water tank and gas concentrations to atmospheric conditions. The main input data used by the programme are listed in Table 3.

TABLE 3: Input data for the WATCH programme (Arnorsson, et al., 1982)

CHEMICAL DATA	
Water samples:	pH/°C, SiO ₂ , B, Na, K, Ca, Mg, Fe, Al, NH ₃ , ΣCO ₂ , SO ₄ , ΣH ₂ S, Cl, F, dissolved solids
Steam samples:	CO ₂ , H ₂ S, NH ₃ , N ₂ , O ₂ , H ₂ , CH ₄ , and Na or Cl to check dryness of steam
PHYSICAL DATA	
Wet-steam wells:	Sampling pressure and discharge enthalpy
Hot water wells and springs:	Discharge temperature
Data which are desirable:	Downhole temperature of wells, aquifer inflow and discharge rates of wells and hot springs

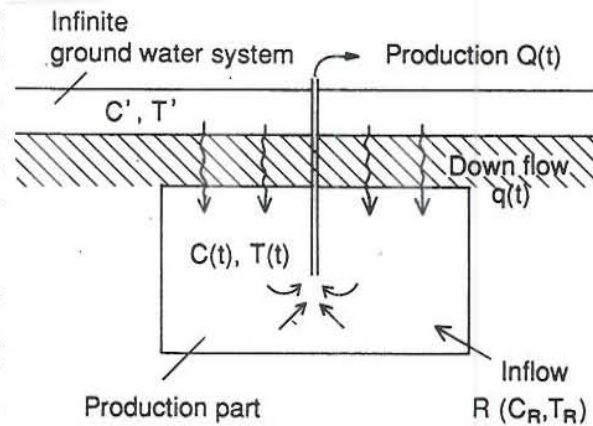
Also necessary were some assumptions regarding the sampling pressure because in some cases it is not available. In the case of samples collected at elevated pressures, a sensitivity study was performed to estimate changes due to 1-2 bar error in the sampling pressures. The study showed that this difference does not affect the results. Therefore the sampling pressure was either taken as the average of the separator pressure between the sampling dates reported, or the WHP which is the same or close to the separator pressure. An important observation is that usually the sampling pressure for the gas samples is reported as the measured pressure in the collection device connected to the steam line, but the real sampling pressure is that of the cyclonic separator (Armannsson, pers. comm.).

In the corrections of the water tank samples to weirbox conditions, a simple statistical analyses was also necessary in order to know the accuracy of the correction. In general, the scattering with this procedure becomes lower than that if the water tank sample was not changed to atmospheric conditions. These differences range between 2-4 %.

3.7 Simple lumped parameter model

Simple lumped reservoir models are useful for estimating some important geometric parameters of a reservoir and for predicting future changes in pressure, temperature and chemistry. One application of these models is the estimation of cooling in a geothermal reservoir due to inflow of colder fluids. The data needed is the monitoring of the chemical concentration of the discharge water and the flow rate during the production time. Usually the decline in chemical composition is believed to be the result of colder fluids seeping into the production part of the reservoir, partially as internal flow in some wells and partially through fractures extending to the surface. A typical example of such application is presented in Bjornsson et al., 1994. The lumped model is shown in Figure 3. It consists of an infinite groundwater aquifer with a water temperature

T' and solute concentration C' . The production part of the reservoir has a volume V , variable temperature $T(t)$ and chemical concentration $C(t)$, with an initial temperature T_o and concentration C_o . The inflow from the outer and deeper parts of the geothermal system is R (kg/s) with temperature T_R and concentration C_R . A variable production of Q (kg/s) starts at time $t = 0$, and also the down-flow of groundwater is variable. This model can also be used to estimate the reservoir volume where the mixing of geothermal water and cold groundwater takes place, given that the reservoir porosity is known. In the model the base inflow, R , is assumed constant with some chemical composition and temperature and represents the hot part of the production induced recharge in addition to the natural recharge, whereas the colder down-flow is variable and represented by $q(t)$ (see Figure 3).



OS 94.01.0013 GAx

FIGURE 3: The simple model used for simulating down-flow of colder groundwater (from Bjornsson et al., 1994)

The equations describing the response of the model are mathematical solutions of differential equations describing the conservation of the mass of a given chemical substance and the conservation of energy. These depend on the properties of the water and the rock formation, like the density ρ_v and heat capacity of water c_v , the porosity Φ of the rocks in the production part of the system and the volumetric heat capacity ρ_c of the reservoir rocks. The governing equation in terms of the chemical concentration for the lumped model is

$$C_i \approx C_{i-1} e^{-\alpha Q_i \Delta t_i} + \frac{(Q_i - R) C' + R C_o}{Q_i} (1 - e^{-\alpha Q_i \Delta t_i}) \quad \text{where } \alpha = 1/(V \rho_v \Phi) \quad (10)$$

for $i = 1, 2, \dots$; and the governing equation for the temperature of the produced water is

$$T_i \approx T_{i-1} e^{-\beta Q_i \Delta t_i} + \frac{(Q_i - R) T' + R T_o}{Q_i} (1 - e^{-\beta Q_i \Delta t_i}) \quad \text{where } \beta = \frac{c_v}{V(\rho_c)} \quad (11)$$

for $i = 1, 2, \dots$; α and β are constant properties of the reservoir and V is the volume of the mixing part. The name of the game is, therefore, to use the known histories of produced fluid temperature $T(t)$, the chemical concentration, $C(t)$, and the production, $Q(t)$, to find the three unknowns, α , β and T' .

4. RESERVOIR EVALUATION

4.1 Chemical changes with time

Several chemical species and ratios were plotted against time using the chemical data collected in the wells from the start of exploitation in 1975 to the present. Almost all the wells show a trend of dilution in the reservoir water chemistry. Only one well showed a tendency of salinity increase. Liquid enthalpy wells show almost constant gas content through the years whereas the two-phase high enthalpy wells show a marked increase in gas concentration.

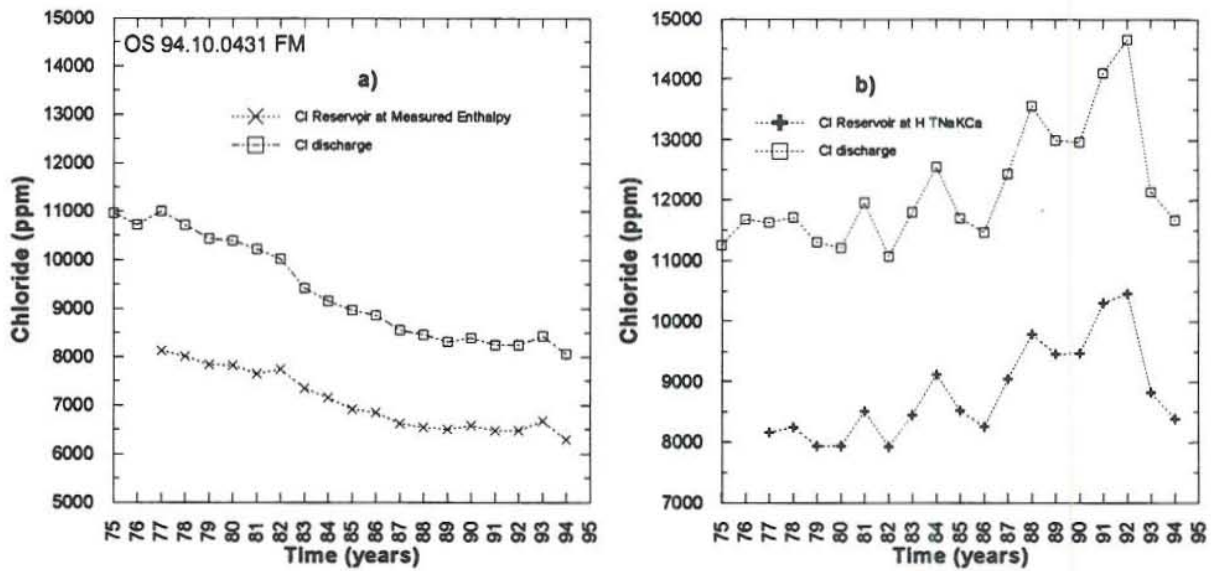


FIGURE 4: The history of discharge and reservoir chloride concentrations in a) AH-1, and b) AH-6

In order to give a general overview of the evolution of water chemistry, in Ahuachapán, two wells were selected as representatives of the different reservoir behaviour observed. These are well AH-1, which was chosen for its marked tendency to produce more diluted waters and also for its low discharge enthalpy. The other was well AH-6 for its progressive and unique tendency to produce more saline fluid and for its evolution through the years to higher enthalpy discharge. The chloride history of these two wells is shown in Figure 4. Both the discharge concentration and the reservoir concentration according to Equations 3 and 4 are shown. The reservoir chloride content for well AH-1 has declined from almost 8000 ppm in the early years of production to 6500 ppm this year. The decline was gradual until 1987 but has shown some stabilization in the last few years. This represents a dilution of 19%. Well AH-6, on the other hand, shows in spite of some scattering behaviour a clear trend towards increased reservoir chloride content. Only in the last two years or so are lower values observed, than in the previous years. Such changes could be related to a cyclic chemical behaviour and are possibly related to fluctuations in the water mass flow rate.

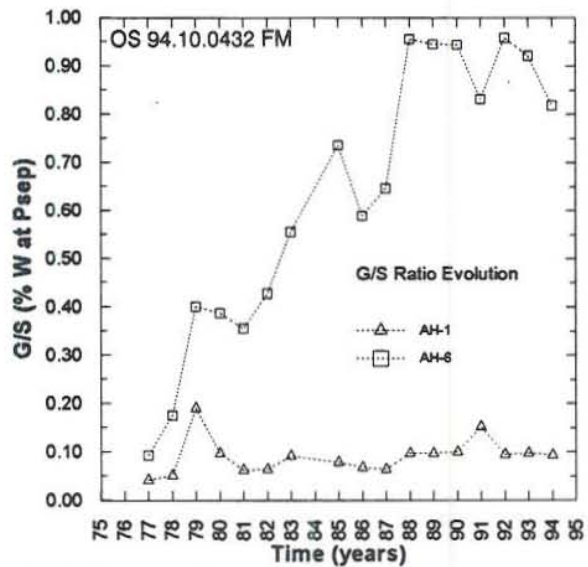


FIGURE 5: Gas-steam ratio history for the representative wells; the G/S is in weight % at separator pressure

The gas content in these two wells has also changed (Figure 5). Well AH-1 shows almost a constant gas concentration compared to well AH-6 which shows an abrupt tendency to increase the gas content. Note that when well AH-6 started its production, the gas content was almost the same as in well AH-1.

This behaviour is clearly related to the thermodynamic conditions of the main feedzones of the wells, which change with time. That is, a liquid feedzone with a low gas content is still not affected by gas fractionation (AH-1), whereas a two-phase feedzone becomes more gas enriched with time due to boiling (AH-6). Using the difference between the quality of the feedzones in the producer wells related to the enthalpy content, it is possible to classify them in several groups according to the specific range of gas content. This classification of high and low enthalpy wells is demonstrated in Figure 6. The remaining 4 wells not shown in this figure are classified as moderate enthalpy wells and have gas concentration between the two groups in Figure 6.

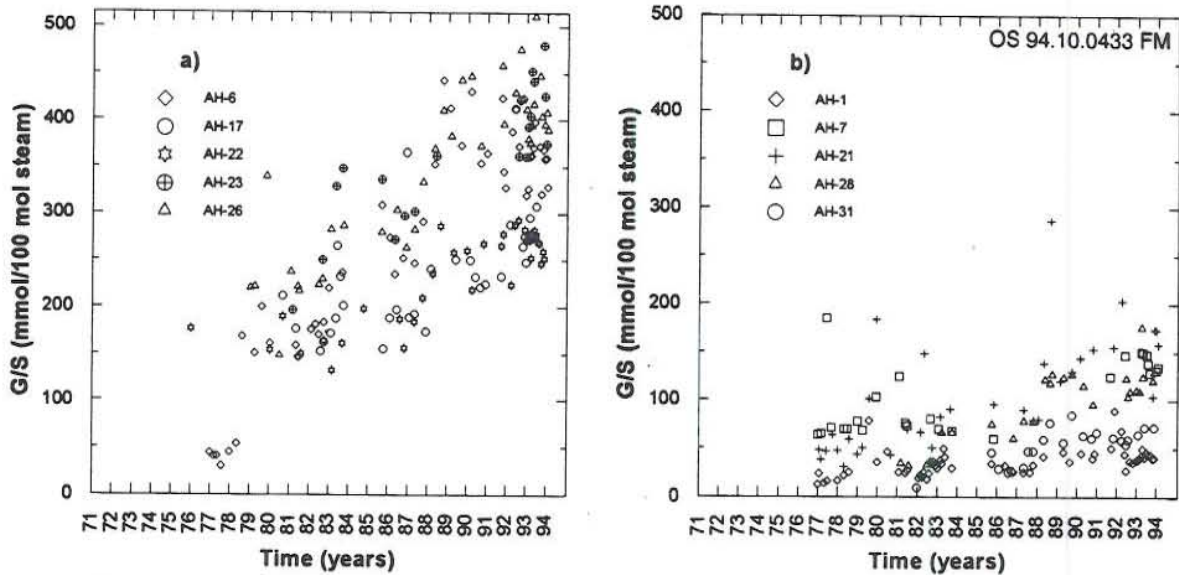


FIGURE 6: Classification of high and low enthalpy wells based on the gas content evolution, a) high-enthalpy wells, and b) low-enthalpy wells; gas-steam ratio in mmol/100 mol steam

In all geothermal systems related to volcanic activity, the main gas is generally CO₂, with 90% or more of the total gas composition. But in general description, it is possible to classify the wells with a high enthalpy discharge, as higher CO₂ and with less H₂S and N₂ content, than that for the low-enthalpy wells.

4.2 Processes in the reservoir

4.2.1 Enthalpy-chloride mixing model

Figure 7 shows a mixing model for the Ahuachapán wells. The reservoir chloride content and the measured discharge enthalpy for the low- and moderate-enthalpy wells is shown, but for the high-enthalpy processes the enthalpy provided by the Na-K-Ca geothermometer is used. The model shows two reservoir processes, 1) typical dilution (well AH-1), which changes the enthalpy and chloride to lower values with time, and 2) the boiling process shown by well AH-6, with a cooling trend effect (according to the Na-K-Ca geothermometer) due to boiling with decreasing enthalpy (liquid aquifer) and concentrated reservoir chloride content.

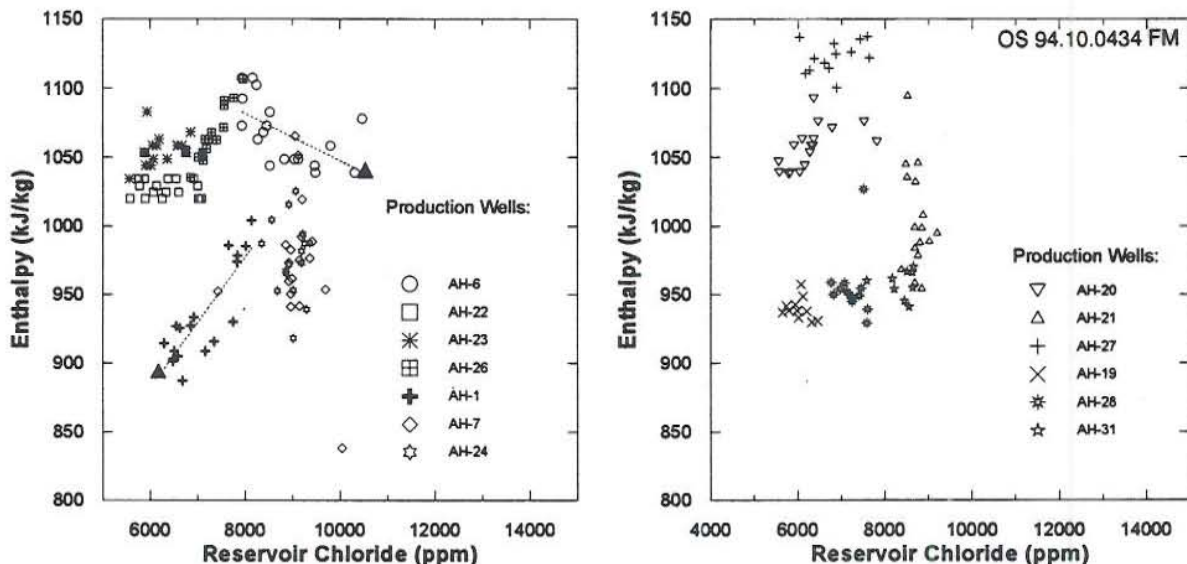


FIGURE 7: Enthalpy-chloride mixing model for production wells, the arrows show the dilution of well AH-1 and the chloride enrichment in well AH-6 with time

In Figure 7 the main tendency with time is illustrated with arrows. All the producer wells (except AH-17 which is a dry steam well, and AH-32 that does not have chemical history data) were plotted in search for such trends. Some wells, such as AH-19, AH-28 and AH-31, show an almost constant enthalpy and a little decrease in the reservoir chloride content and well AH-22 shows a definite decrease with time in chloride content but constant enthalpy. On the other hand, wells AH-23 and AH-27 have shown some decrease in enthalpy and also chloride. Finally, wells AH-7, AH-20, AH-21, AH-24 and AH-26 show a marked uniform decrease in enthalpy and also in chloride, very similar to well AH-1. With the methodology presented here it becomes complicated to describe the origin of the different chemical histories due to boiling, dilution or other reservoir processes, because of the complex behaviour that each well can show during exploitation.

The present analysis can be considered as a qualitative description. In the vicinity of a particular well one can assume several mechanisms to explain the different tendencies described above. Figure 7 also shows the major boiling path connecting the chloride and the enthalpy evolution of well AH-6. Boiling, heat transfer from the rock and steam addition can change the enthalpy without changing the chloride (LBL, 1988). Additional heat transfer from the rocks can also be followed by some evaporation. Wells AH-19, AH-28 and AH-31 could be related to light evaporation, but the chloride concentration does not have a wide variation with time. Therefore these wells seem to be the most stable ones in the mixing model. Well AH-22 is another that can be related to some evaporation process but shows also some stability. If mixing with relatively cold waters occurs, then compositions move from the boiling trend like in well AH-6 towards a dilution trend like the one shown for well AH-1 in Figure 7. There seems to be another pathway of different fluid that moves to less reservoir chloride values but with some scattering in the enthalpy variations, as for wells AH-7 and well AH-24. It is also possible that coupled processes are occurring in the reservoir such as mixing of different fluids followed by conductive heating. These processes will lead to complicated relations between enthalpy and fluid concentrations.

It is of interest to include the Chipilapa geothermal field and the El Salitre hot springs into the mixing model study. Figure 8 shows the relation between these thermal waters along with those Ahuachapán wells affected by dilution with relatively colder waters. Unfortunately, little chemical data is available from the Chipilapa wells. Therefore, mainly data from the last wells drilled is included in this model. A representative chemical composition for each well was estimated by using the measured enthalpy for the calculation of the reservoir chloride composition. Several data sources were used (Montalvo, 1991; CFG, 1992; CEL, 1994).

The values for the reservoir chloride varies from 1756 to 3482 ppm for wells CH-8 and CH-9, and the enthalpy for wells CH-7 and CH-D varies between 745 and 1010 kJ/kg. New data for the El Salitre hot springs is also plotted, in Figure 8, showing the natural decline of chloride and temperature with time.

Figure 8, shows a clear dilution line between wells AH-1, AH-7 and AH-24, and wells CH-7, CH-8 and CH-9. The wells CH-7b and CH-D present a light displacement by anomalous enthalpy values, that could be overestimated, probably due to the short period of discharge. Another dilution line could possibly connect the Ahuachapán wells and the El Salitre hot springs.

4.2.2 Chemical and thermodynamic indicators

The different responses of the Na-K-Ca and quartz geothermometers combined with the enthalpy of each well, provide indications on fluid state and on fluid

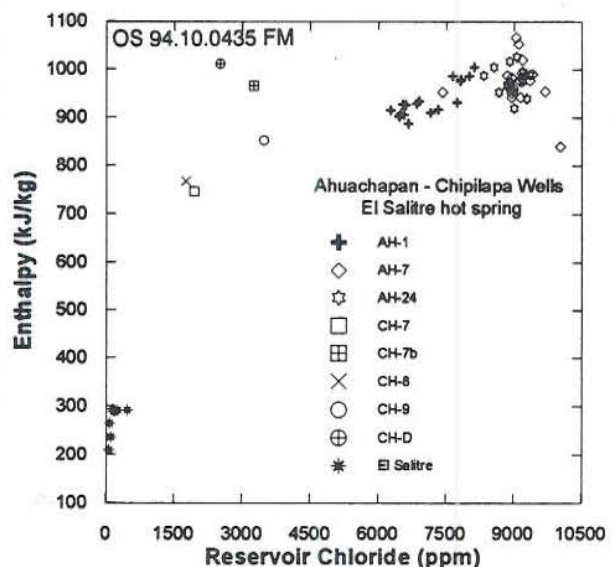


FIGURE 8: Mixing model showing the relation between Chipilapa wells, El Salitre hot springs and Ahuachapán more diluted wells

temperature near and far from the wells. The enthalpy evolution of Ahuachapán wells revealed by this comparison is summarized for all the wells in Table 4 and furthermore shown in Figure 9, for wells AH-1 and AH-6.

TABLE 4: Main thermodynamic processes occurring in Ahuachapán production wells

Wells	Prevalent order	Indicated process
AH-1, 7, 19, 21, 24, 28 and 31	$H_{Na-K-Ca} > H_{SiO_2} > H_m$	Mixture of cooler more diluted water
AH-6, 22, 23, 26, 20 and 27	$H_m > H_{Na-K-Ca} > H_{SiO_2}$	Boiling during flow to the well

H_m = measured enthalpy;

$H_{Na-K-Ca}$ = enthalpy at Na-K-Ca geothermometer;

H_{SiO_2} = enthalpy at quartz geothermometer.

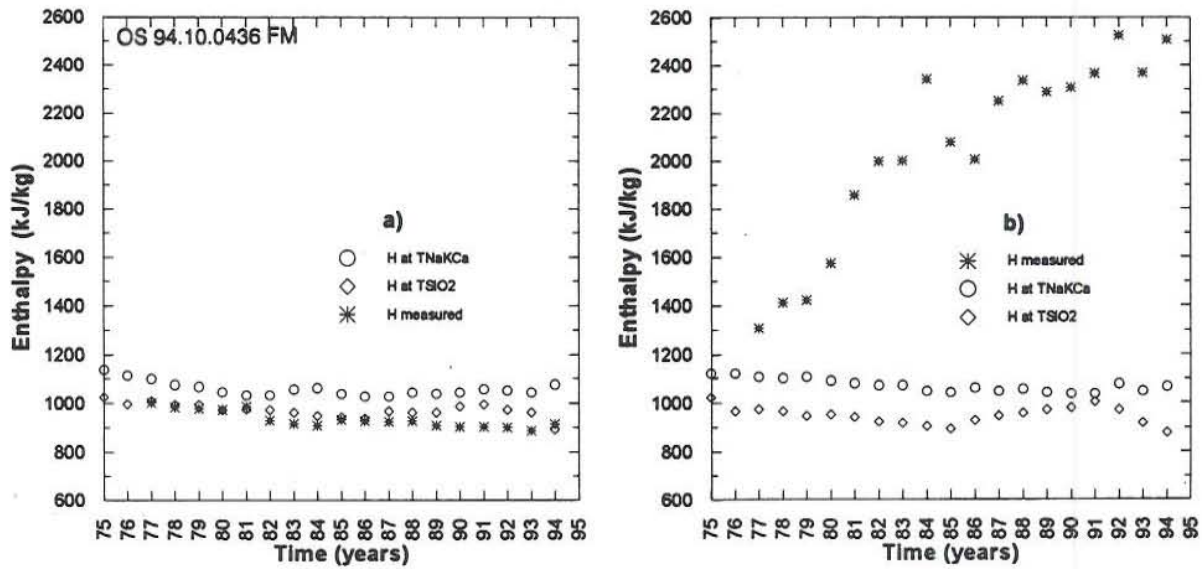


FIGURE 9: Enthalpy-geothermometry comparison showing the behaviour of a) well AH-1, and b) well AH-6

Boiling lowers fluid temperature within expanding boiling zones with progressively decreasing pressure (drawdown), and the fluid state corresponds to the two-phase liquid-vapour curve. The near well fluid is cooled by the boiling, and the heat is transferred to the fluid from the reservoir rocks, probably resulting from flashing flow in fractures (that is the case of Ahuachapán). That, on a large scale, may behave like a uniform matrix but may also allow segregation of liquid and vapour (LBL, 1988). According to Table 4, six wells are affected by local boiling, but the rest (seven wells) produce diluted waters.

When cooler water enters the well and mixes with the reservoir fluid close to the well (or in the well), the water enthalpy (actual temperature) and the silica temperature will decrease but little change occurs to the Na-K-Ca temperature. This mixture does not necessarily cause re-equilibration but will give lower silica temperature because of dilution. If the mixing occurs in the reservoir far enough from the well to allow silica equilibration, the enthalpy sequence will be $H_{Na-K-Ca} > H_{SiO_2} > H_m$. This is the case of well AH-1, during the period 1975-88, when the silica temperature and the temperature from the measured enthalpy are almost identical (Figure 9). This was also observed in previous work (Steingrímsson et al., 1991; Truesdell et al., 1989) where the initial fluid chemistry in the field was assumed to indicate mixing in the reservoir related to some colder less saline water. This process is not seen in the rest of the wells, where the most common trend presented in the enthalpy history is a colder water inflow into the well, probably due for the lowering cold

water/hot water interface as pressure drops. A special case is the behaviour of well AH-21, where the enthalpy sequence has changed from $H_{NA-K-Ca} > H_m > H_{SiO_2}$ in the beginning to $H_{NA-K-Ca} > H_m \approx H_{SiO_2}$ and finally to $H_{NA-K-Ca} > H_{SiO_2} > H_m$. Other cases can occur by combination of these processes producing ambiguous indications, so here it is concluded that some boiling took place near the well in the early period, but at present the well can be affected by mixing and probably also boiling. Note that there is a figure showing this in the Appendix and also for the other wells (Montalvo, 1994).

4.2.3 Field-wide variations

The chemical data from the wells and the calculated enthalpies have been contoured on maps in order to study the chemical and thermodynamic properties of Ahuachapán with time and space. Here we will discuss the distribution of reservoir chloride, silica temperature, Na-K-Ca temperature and gas-steam ratio. A comparison is made between the reservoir chloride distribution in 1978 and 1993 in Figure 10.

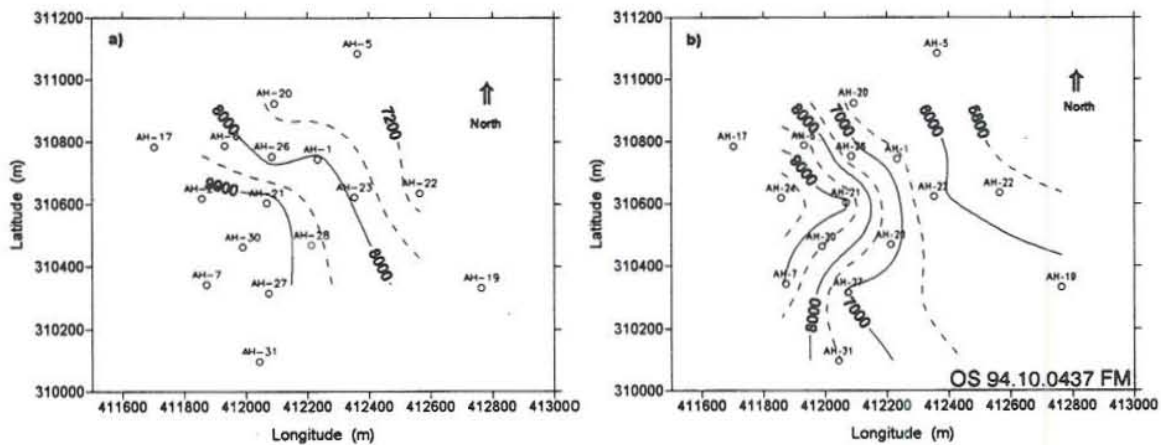


FIGURE 10: Reservoir chloride distribution (ppm), a) in 1978, b) in 1993

The reservoir chloride distribution (before 1975) in the early exploitation years showed a smooth distribution, with the high values around 9000 ppm in the southwestern part of the field, about 8000 ppm in the centre and the lower values close to 7000 ppm in the eastern part of the field (see Appendix, Figure 9, showing reservoir chloride in the natural state). In 1978, clear changes started field-wide, mainly in the wells located to the north showing a slight decrease of chloride content, but an increase in some wells located in the centre and the southwestern part of the field can also be observed. In 1993 more evident disturbances are seen in the northeastern and the eastern part of the wellfield with chloride decreasing below 6000-7000 ppm, whereas the western and southwestern part seems to remain at 9000 ppm chloride content. These areas of low and high chloride concentrations can be interpreted as the colder inflow and the hot recharge zones of the reservoir.

The silica temperature distribution is presented in Figure 11. The major change observed is a cooling front developed from 1978 to 1993 in the north and northeast section of the field. The temperature has declined from 223-227 to 216-222°C in the northern part and from 229-230 to 224-228°C in the northeastern part of the field. In the southeastern part the silica temperature has remained constant at around 230-240°C.

Figure 12 shows the Na-K-Ca temperature distribution in Ahuachapán. This geothermometer shows that in 1978 a uniform temperature gradient from about 260°C in the west to little under 240°C in the east part of the field, with a suggested movement of the main flow from the west toward the eastern part and temperatures of 250°C in the centre of the field. Similar observations have been reported for the natural state reservoir

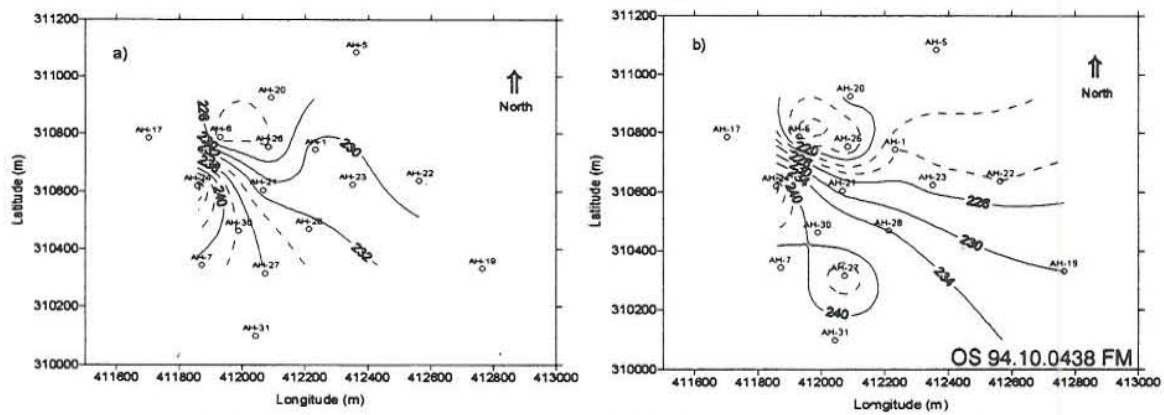


FIGURE 11: Silica temperature distribution ($^{\circ}\text{C}$), a) in 1978, b) in 1993

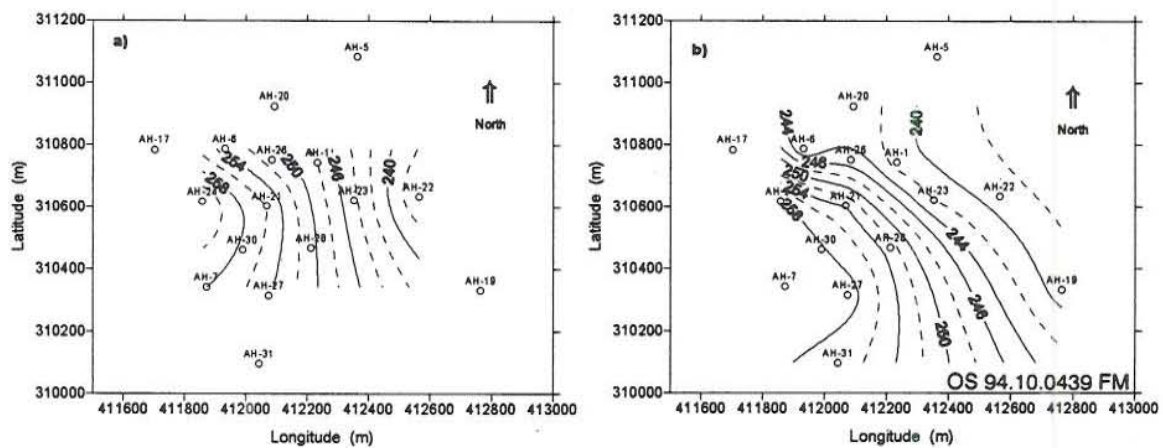


FIGURE 12: Na-K-Ca temperature distribution ($^{\circ}\text{C}$), a) in 1978, b) in 1993

temperatures distribution (Truesdell et al., 1989). In 1993 the Na-K-Ca thermal front seems to be a little bit modified in the southwest and the north part of the field, due mainly to some cooling in the north from 248-250 to 242-244 $^{\circ}\text{C}$ and a possible heating in the southwest of around 2 $^{\circ}\text{C}$. This minor heating might be due to recharge of hotter fluid into the production field.

Figure 13 illustrates the changes in the distribution of gas-steam ratios for the wells. This ratio is particularly sensitive to the development of two-phase zones in the reservoir, and should be compared with the variations of the measured enthalpy distribution shown in Figure 14. In 1978 the highest gas-steam ratios are in the north which agrees with the enthalpy distribution for this year (natural state with an early appearance of boiling), reflecting a steam zone around well AH-6, trending towards the centre of the well field. The gas ratio and enthalpy distribution in 1993 are clearer, showing the close relation between the expansion of boiling zones, and the increase in the gas-steam ratio.

4.2.4 Reservoir flow-weighted averages

In order to observe the general behaviour of the reservoir fluid, flow-weighted averages were calculated using monthly averages of the total flow rate (steam and water), reservoir chloride, measured enthalpy and calculated enthalpy from the Na-K-Ca geothermometer for all the wells. The governing equation of these calculations is shown in Chapter 3.2 and in the supplementary Appendix of this report a full listing is given on the results of these calculations (Montalvo; 1994).

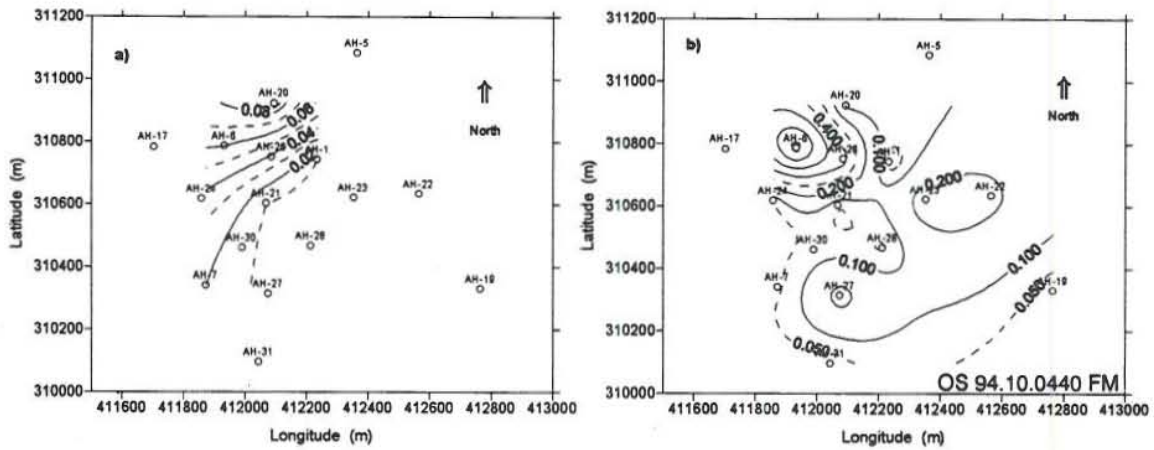


FIGURE 13: Gas-steam ratio distribution (%W at separated pressure), a) in 1978; b) in 1993

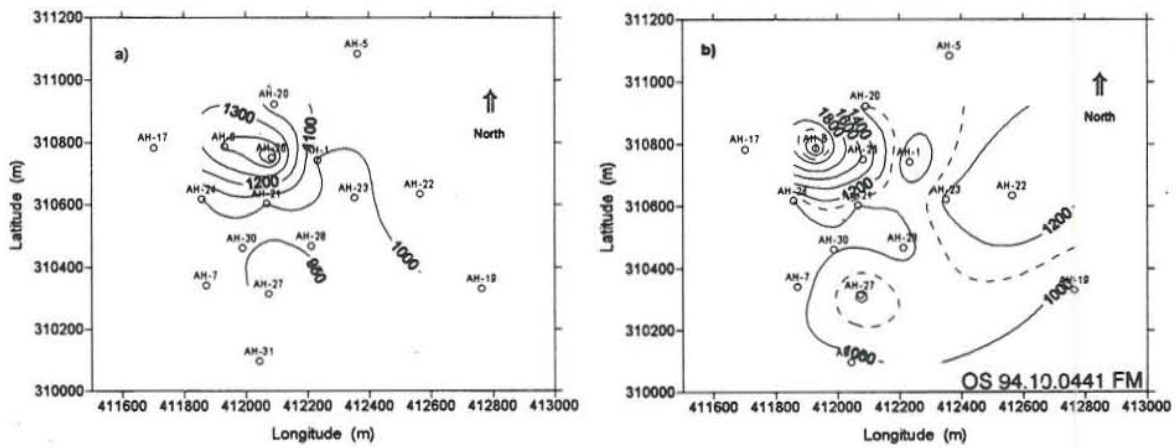


FIGURE 14: Measured enthalpy distribution (kJ/kg), a) in 1978, b) in 1993

The flow-weighted averages for the reservoir chloride and Na-K-Ca-enthalpy are shown in Figure 15 for all the wells and Figure 16 shows the flow-weighted discharge enthalpy trend for the lower enthalpy wells. According to these figures the flow-weighted chloride is decreasing with time, the enthalpy calculated from Na-K-Ca geothermometer is fairly constant whereas the average discharge enthalpy of the low temperature wells shows an increase up to the year 1980 when it starts declining again until present.

The chloride decline during the 20 years period shown in Figure 15 is around 1000 ppm indicating an inflow into the reservoir of a low salinity fluid. This fluid mixes with the higher salinity reservoir fluid and dilutes it. The constant behaviour of the Na-K-Ca thermometer values indicates that the chemistry (temperature) of the hot recharge to the reservoir has remained constant. Finally, the decreasing trend in the enthalpy of the low enthalpy wells (Figure 16) indicates that the low salinity fluid that dilutes the reservoir fluid is colder than the geothermal recharge. The most likely source of the low salinity fluid recharge is the saturated aquifer that overlies the geothermal reservoir. The salinity of the saturated aquifer is around 400 ppm and its temperature is around 120°C.

4.3 Cold water inflow estimation

The simple model presented in Chapter 3.7 was used to simulate the flow-weighted chlorine and enthalpy measurements in Figures 15 and 16. The basic assumptions for the two inflows into the mixing model, shown in Figure 3, are:

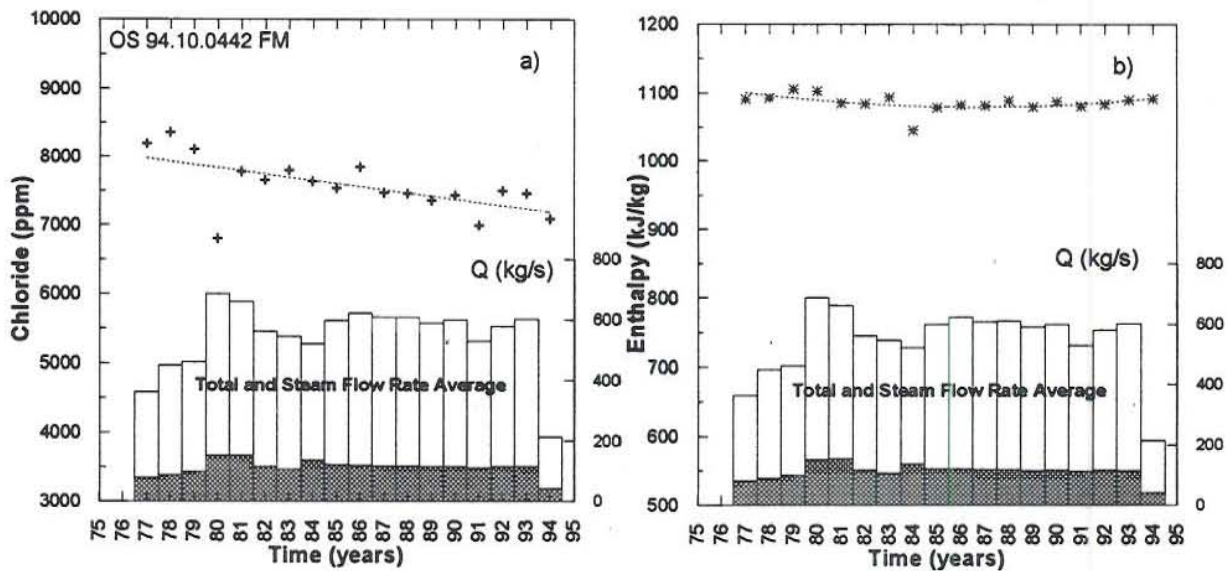


FIGURE 15: a) The flow-weighted chloride content and, b) flow-weighted Na-K-Ca reservoir enthalpy for all the Ahuachapán wells

- 1) The colder and less saline recharge to the reservoir comes from the overlying saturation zone;
- 2) The deep, geothermal recharge has not changed in temperature and salinity during the last 20 years.

In the first phase of the modelling work, only the flow-weighted chloride history in Figure 15 was simulated.

Table 5 shows the lumped reservoir properties used and the value of α which gave the best match between the observed and the calculated flow-weighted chloride. Figure 17a shows the match between observed and calculated chloride data. This data is also shown in the Appendix along with the simulated temperature data.

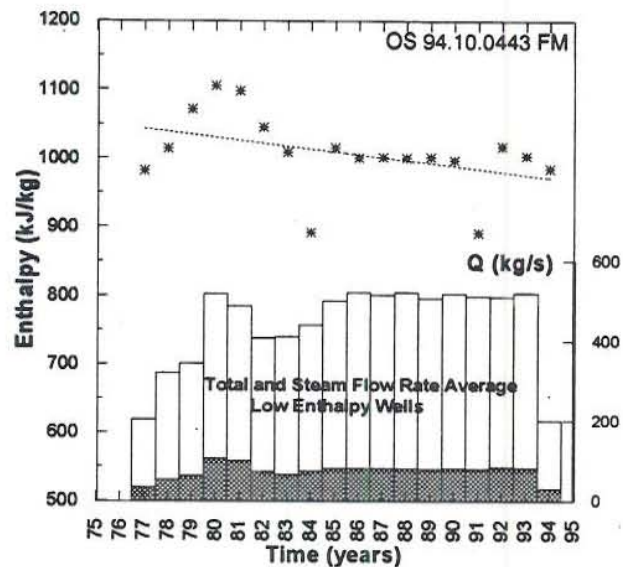


FIGURE 16: Flow-weighted measured enthalpy for the low- and moderate-enthalpy Ahuachapán wells

In Table 5 C' and C_R are the chemical concentrations of the colder down-flow and the deep inflow respectively, R and Q_t are the constant inflow and the average production rate, respectively (in this case fixed), and the others are water and rock properties (see Chapter 3.7). The results indicate a mixing volume of about 0.5 km^3 using a reservoir porosity of 15% and chloride concentration of 1000 ppm for the water inflow from above.

The second phase of the simulation consisted of computing the temperature history of the mixing volume (Equation 11 in Chapter 3.7). Three porosities of 10, 15 and 20% were used for calculating the mixing volume, and consequently the number β in Equation 11. Two temperature values of 130 and 160°C were assigned to the shallow inflow $q(t)$. Table 6 summarizes the results of the calculations and Figure 17b shows the match between observed and calculated temperatures for the model case of the 15% porosity and 130°C shallow inflow temperature.

TABLE 5: Model parameters used for the simulation of the flow-weighted chloride history

Model properties	Mixing volume
$C' = 1000$ ppm	$V\rho_V\Phi = 6.31 \times 10^{10}$ kg
$R = 520$ kg/s (fixed)	$\rho_V = 805$ kg/m ³
$C_R = 8250$ ppm	$\rightarrow V\Phi = 7.84 \times 10^7$ m ³
$\alpha = 1.58 \times 10^{-11}$ 1/kg	$\Phi = 0.15$
Average $Q(t) = 581$ kg/s	$\rightarrow V = 0.52$ km ³

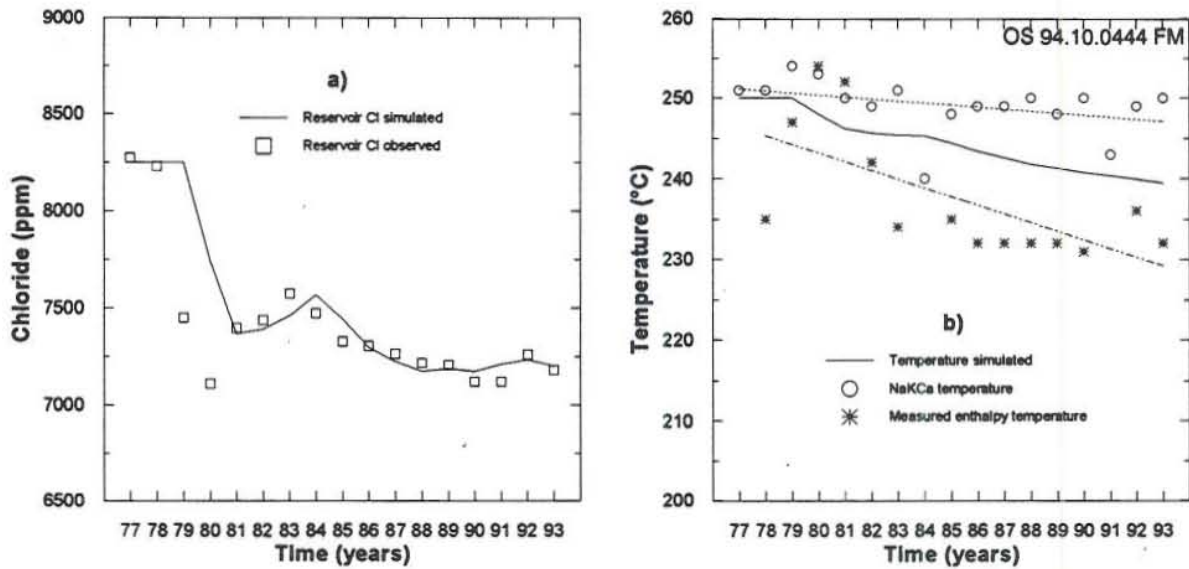


FIGURE 17: Observed and calculated flow-weighted, a) chloride concentrations, b) temperatures

TABLE 6: Calculated cooling by the simple lumped parameter model, also listed are the rock-water properties used in the model

Φ	0.1		0.15		0.2	
V (km ³)	0.784		0.523		0.392	
β (1/kg)	6.76×10^{-5}		1.01×10^{-4}		1.35×10^{-4}	
T' (°C)	130	160	130	160	130	160
T_{1976} (°C)	250	250	250	250	250	250
T_{1993} (°C)	241.9	244	239.4	242.1	237.6	240.7
ΔT (°C)	8.1	6	10.6	7.9	12.4	9.3
Δh (kJ/kg)	34	25	45	33	52	39
$C_w = 4200$ J/kg°C	$C_r = 800$ J/kg°C		$\rho c = 2.5 \times 10^6$ J/m ³ °C		$T' = 130-160^\circ\text{C}$	
$\rho_w = 805$ kg/m ³	$\rho_r = 2900$ kg/m ³		$T_R = 250^\circ\text{C}$		$R=520$ kg/s, $Q=581$ kg/s	

A comparison between the calculated and the measured flow-weighted enthalpy gave best fit for the inflow temperature of 130°C and 15% porosity resulting in average cooling of 11°C and enthalpy decline of 45 kJ/kg. The model case of 20% porosity and 130°C inflow temperature also showed a good match.

Note that Figure 17 shows both the flow-weighted field average for the Na-K-Ca-temperature and the measured enthalpy temperature. The calculated, mixing volume temperature is between these curves. This average model temperature is assumed reasonable for the following reasons:

- 1) The Na-K-Ca geothermometer needs long time to equilibrate with the formation temperature and is, furthermore governed by the massive, deep recharge. This may lead to overestimation of the mixing volume temperature.
- 2) The reservoir boiling causes additional cooling in the mixing volume, compared to what would happen if only the colder, shallow recharge took place.

A sensitivity study on the previous mixing model still needs to be done. For example lowering the shallow recharge chloride requires either high fraction of the deep recharge to the total flow or high salinity. However, this will not change the major conclusion that the two measured histories of flow-weighted chloride and production temperature constrain the shallow recharge to be around 10-20% of the total mass produced.

Finally, it should be emphasized that the above model simulates Ahuachapán production data. The deep recharge of more than 500 kg/s should, therefore, not be mixed with the deep recharge of 250 kg/s estimated in natural state simulations (LBL, 1988; ELC, 1993). The higher recharge in the production model is due to the reservoir pressure drawdown and mass produced from storage and the deeper reservoir boundaries.

5. REVISED CONCEPTUAL MODEL

A hydrologic conceptual model of the Ahuachapán field is presented in Figure 18. Similar models have been published before (Steingrímsson et al., 1991; Aunzo et al., 1991; Truesdell et al., 1989), but the new model shows some modification mainly regarding the movements of the different types of chemical fluids into the reservoir and regarding the mixing-boiling process developed with time in the well field due to exploitation. These modifications are based on the various methodologies applied in this report.

A description of the model in Figures 18 is as follows. An up-flow of saline, high temperature fluid (around 250°C and up to 8000 ppm of chloride) is believed to take place underneath the volcanoes south of the well field (probably close to Laguna Verde). From the up-flow zone, the fluid flows laterally towards the north, all the way to the El Salitre hot spring area with branches of flow towards Ahuachapán and Chipilapa.

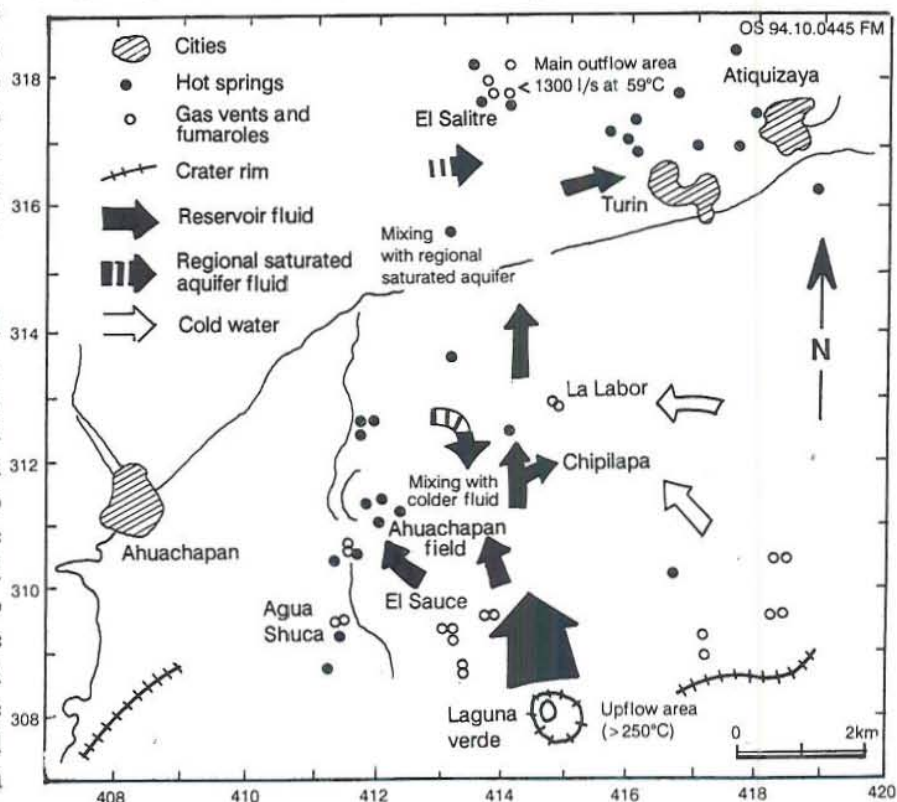


FIGURE 18: Conceptual model of fluid flows in the Ahuachapán field under actual exploitation conditions

The flow towards Ahuachapán seems to be differentiated into two flow paths, before it enters the production area. One inflow (recharge) zone is in the southwestern part of the well field, but the other seems to be in the southeast part. The recharge to the southwestern part of the well field has the chemistry of the Laguna Verde up-flow zone whereas the recharge to the southeastern part has undergone a dilution with colder and less saline fluid before or as it enters the well field. The fluid diluting the recharge is believed to originate in the saturated aquifer, which overlies the geothermal reservoir and has water temperature of approximately 130°C and salinity of 1000 ppm of chloride, according to the simple model described in Chapters 3.7 and 4.3.

The recharge to the Chipilapa area has probably undergone even more dilution than the southeastern part of Ahuachapán recharge, as the chloride content of Chipilapa fluid is only 3000-4000 ppm. The hydrological connection between the El Salitre and Ahuachapán is obvious if one looks at the discharge history of El Salitre prior to the exploitation of Ahuachapán. The hot springs yielded initially around 1300 l/s of 70°C and about 500 ppm of chloride hot water. Now, 20 years later after considerable pressure drawdown in Ahuachapán field, the flow rate at the El Salitre is only about 300 l/s or less, and the temperature around 50°C and there is less than 100 ppm of chloride in its water discharge (LBL, 1989; CEL, 1994).

The main differences between this conceptual model and the one presented by the LBL group (1989) is that the mixing with colder fluid illustrated in the previous model is a little bit displaced from the north to the northeastern part of the field and that the colder recharge fluid originates from the saturated regional aquifer. Another important difference is that the recharge to the saturated aquifer is affected by this dilution of fluids in the southeastern part of the field but the recharge to the southwestern part is not (see Figure 18). Also the main boiling zone shows an expansion trend from the north-northwest (AH-6 and AH-17) to the centre of the field, and there are two more boiling zones identified in the south-southeast (AH-22) and south-southwest (AH-27). This means that at the actual state all the field is affected by mixing and boiling processes. A cross-section showing the main geological formations and the representation of this process is illustrated in Figure 12 in the Appendix (Montalvo, 1994).

5. DEPOSITION PROBLEMS EVALUATION

To estimate the deposition risk in producing wells, speciation calculations were made using all analytical chemical data available for the well fluids over the last five years. The analytical results for well fluids for AH-1 and AH-6 are presented in the Appendix. So are the results of quartz, calcite and anhydride saturation

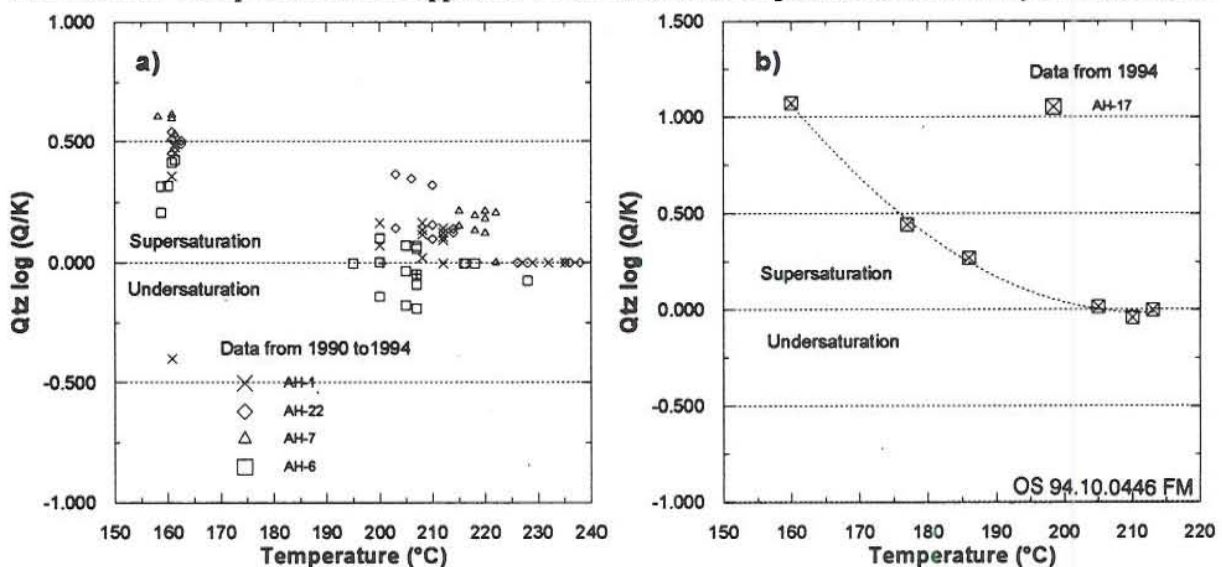
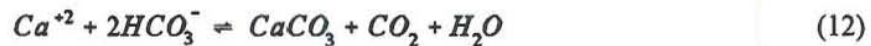


FIGURE 19: a) Quartz saturation index for reservoir and well head pressure conditions for selected wells, and b) saturation index evolution for well AH-17

index calculations for fluids from selected wells, which are plotted in Figures 19, 20 and 21, respectively. The possible evolution of quartz scaling in well AH-17 is shown in Figure 19b and that of calcite scaling in AH-32 in Figure 20b. Also shown for comparison is a similar curve for fluid from well SV-09, Svartsengi, Iceland, where scaling is a problem. In the Appendix the chemical analysis for wells AH-1 and AH-6 are presented and results for quartz, calcite and anhydride saturation index for selected wells (Montalvo, 1994).

In general, all the fluids are close to equilibrium with quartz and during adiabatic boiling they reach the wellhead in a state where there is no risk of quartz scaling. There is no evidence of calcite scaling at wellhead conditions in the last few years. A small degree of supersaturation observed for well AH-7 fluid is probably due to analytical error. The overall process of calcite scaling can be described by the equation



Therefore, scaling is increased by increase in Ca^{+2} , changes in pH (increases with high pH) and removal of CO_2 which occurs upon boiling. The last process is by far the most important in geothermal wells.

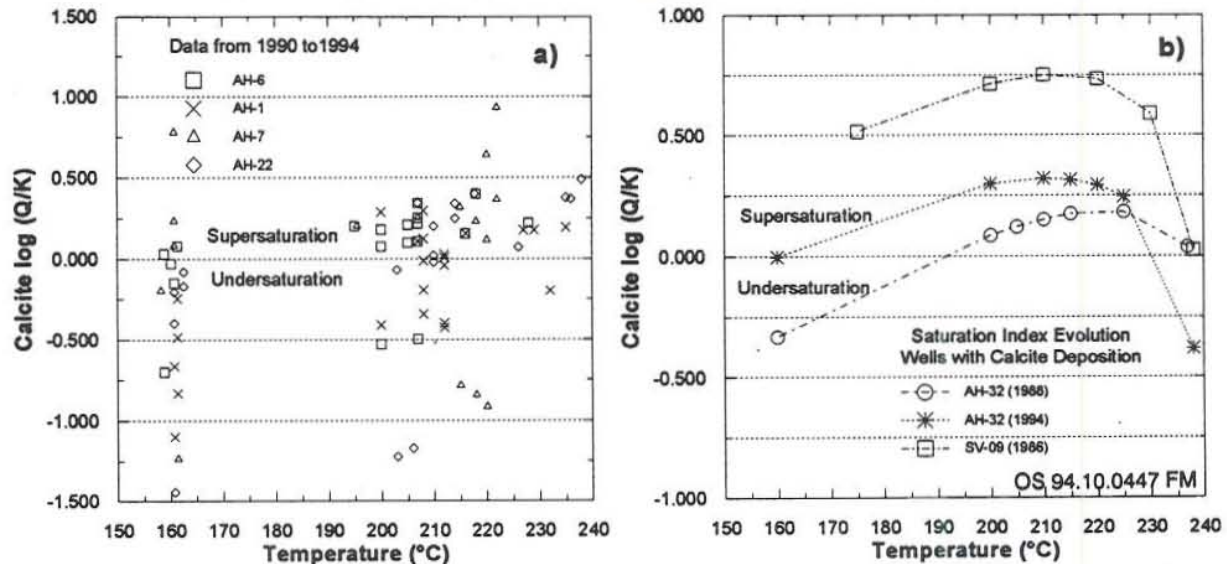


FIGURE 20: a) Calcite saturation index at reservoir and well head pressure conditions for selected wells, and b) calcite scaling potential comparison between wells AH-32 and SV-09

The changes shown in Figure 20b are mainly due to supersaturation due to boiling even though attendant increase in Ca^{+2} and pH may play a small part. Relatively more CO_2 is removed from well SV-09 than from well AH-32 fluid upon boiling and this is the probable reason for the former's greater calcite scaling potential.

Previous reports have mentioned that problems related to the deposition of anhydride could occur in the reservoir, mainly in well AH-6 (Electroconsult, 1993). For this reason the saturation state of this mineral in the reservoir was evaluated (Figure 21). The figure shows low risk of anhydride deposition in the reservoir, almost all the results are in under-saturated conditions.

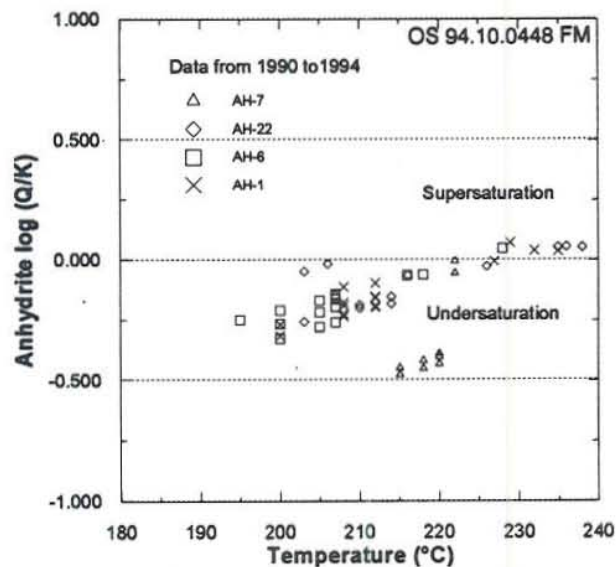


FIGURE 21: Anhydride saturation index at reservoir conditions for selected wells

7. CONCLUSIONS AND RECOMMENDATIONS

7.1 Conclusions

The main results of this study can be summarized as follows:

1. A data base of around 2800 fluid samples from the Ahuachapán wells has been established and filtered for possible errors due to sampling or analysing ambiguities.
2. The plotting of chemical concentrations with time shows a trend of dilution in the reservoir water chemistry, with the exception of one high enthalpy well. Liquid-enthalpy wells show almost constant gas content through the years whereas high-enthalpy wells, producing from boiling regions, show a marked increase in gas concentration. These changes are correlated with recharge of diluted fluid to the reservoir and gas fractionation in the boiling zone.
3. Enthalpy - chloride mixing models, furthermore, show that the lower concentration fluid recharge is colder than the reservoir fluid, resulting in decreasing enthalpy and chloride concentration with time for the liquid enthalpy wells. Geothermometers indicate that some of the cooling is also due to boiling.
4. Comparison of measured enthalpy and enthalpy deduced from geothermometers shows that six of the Ahuachapán wells are presently affected by local boiling and seven with dilution by colder fluid, but two of them show signs of increasing reservoir enthalpy.
5. A study on the distribution of reservoir thermodynamic and reservoir properties shows chloride dilution and cooling in the north and northeast section of the present well field. The west and southwestern part, however, remain stable in fluid concentration and temperatures. These areas of low and high chloride concentrations and reservoir temperatures are interpreted as colder inflow zones and hot recharge zones to the reservoir, respectively. Na-K-Ca geothermometers are even suggesting some heating in the southwestern part.
6. Flow-weighted averages for the reservoir chloride, and enthalpy based on measured values and estimates by geothermometers, show that the mean reservoir chloride concentration has changed from around 8000 ppm to 7000 ppm and an average reservoir cooling of 11°C has occurred between 1975 and 1993.
7. A lumped model study, based on the flow-weighted averages, shows that the most likely source of the colder and less saline recharge to the reservoir is the saturated aquifer above. The model predicts that 10-20% of the total production is taken from this zone. It also indicates a 0.5 km³ reservoir volume where the mixing of shallow and deep recharge water takes place.
8. A scaling potential calculation shows that well AH-17 is supersaturated in quartz and well AH-32 in calcite. The other wells all show equilibrium or slight supersaturation with respect to quartz, amorphous silica, anhydride and calcite and are, therefore, assumed to be operational without the risk of scaling in the near future considering the actual chemical conditions.

Finally, it should be stressed that the above study indicates that the majority of the fluid produced from Ahuachapán reservoir is provided by a massive, deep recharge.

7.2 Recommendations

1. In order to optimize the accuracy of the chemical data interpretation, a simultaneous sampling of the water and gas samples at the same conditions is recommended. More specific information about the sampling and chemical analysis procedure is also of value. This will allow more precise results of numerical studies like the ones performed in the WATCH programme.
2. The production strategy in Ahuachapán should be supported by the quality of the fluid produced from wells. This may provide early warning for potential scaling and provide time for appropriate preventive measures if possible.
3. New wells that will be drilled to the south of the present wellfield are expected to develop calcite scaling. Preventive means like large diameter wells (13 3/8" production casings) are recommended in order to lengthen the interval between cleaning operations. Another preventive measure would be the use of inhibitors.

ACKNOWLEDGEMENTS

I would like to express my gratitude to Dr. Ingvar Birgir Fridleifsson, director of the UNU Geothermal Training Programme for making my Fellowship possible, and special thanks to Mr. Ludvik S. Georgsson and Ms. Margret Westlund for providing excellent attention and work conditions during the training.

I sincerely thank Mr. Benedikt Steingrímsson and Mr. Grimur Björnsson, my advisers, for sharing their experience and knowledge on reservoir engineering, and special thanks to Dr. Gudni Axelsson for his assistance in the simple model simulation. I would also thank Dr. Halldor Armannsson and Dr. Jon Orn Bjarnason for useful comments about the geochemical methodologies and WATCH programme utilization.

Finally, I would like express my gratitude to the Comisión Ejecutiva Hidroeléctrica del Río Lempa (CEL), specially to the Superintendencia de Explotación Geotérmica and the Departamento de Ingeniería de Reservorios for giving me the chance to participate in this seminar and also by providing me with all the information used in this work.

REFERENCES

- Arnorsson, S., 1985: The use of mixing models and chemical geothermometers for estimating underground temperatures in geothermal systems. *J. Volc. Geothermal Res.*, 23, 299-335.
- Arnorsson, S., Sigurdsson, S., and Svavarsson, H., 1982: The chemistry of geothermal waters in Iceland. I. Calculation of aqueous speciation from 0°C to 370°C. *Geochim. Cosmochim. Acta*, 46, 1513-1532.
- Aunzo, Z., Laky, C., Steingrímsson, B., Bodvarsson, G.S., Lippmann, M.J., Truesdell, A.H., Escobar, C., Quintanilla, A., and Cuéllar, G., 1991: Pre-exploitation state of the Ahuachapán geothermal field, El Salvador. *Geothermics*, 20, 1-22.
- Bjarnason, J.O., 1994: *The speciation programme WATCH, version 2.0*. Orkustofnun, Reykjavik.
- Björnsson, G., Axelsson, G., and Flovenz, O.G., 1994: Feasibility study for the Thelamork, low-temperature

system in N-Iceland. *Proceedings of the 19th Workshop on Geothermal Reservoir Engineering, Stanford University, USA*, 5-13.

CEL, 1994: *Chemistry discharge of CH-D well*. CEL, Geothermal Resources Division, El Salvador, internal report (in Spanish).

CFG, 1992: *Geoscientific studies and report of reinjection experiments using tracers. Revised conceptual model of Chipilapa geothermal field and feasibility reinjection study*. CFG (Consortio Francés de Geotermia), internal report submitted to CEL (in Spanish).

Campos, T., 1985: Ten years of commercial exploitation of the Ahuachapán geothermal field. *Proceedings of the 7th New Zealand Geothermal Workshop, University of Auckland, New Zealand*, 15-20.

Cuéllar, G., Choussy, M., and Escobar, D., 1981: Extraction-reinjection at Ahuachapán geothermal field. In: Rybach, L., and Muffler, L.J.P. (editors), *Geothermal Systems. Principles and case histories*. John Wiley and Sons Ltd., Chichester, 321-336.

Dipippo, R. 1978: The geothermal power station at Ahuachapán, El Salvador. *Geothermal Energy Magazine*, 6-10, 11-22.

Electroconsult, 1993: *Report of resource evaluation. Feasibility of stabilization programme for the Ahuachapán geothermal field*. Electroconsult, internal report submitted to CEL (in Spanish).

Fournier, R., and Truesdell, A.H., 1973: An empirical Na-K-Ca geothermometer for natural waters. *Geochim. Cosmochim. Acta*, 37, 1255-1275.

LBL, 1988: *The Ahuachapán geothermal field, El Salvador - Reservoir Analysis. Volume I: Text and main figures, Volume II: Appendices A through E; Volume III: Appendices F through I*. Lawrence Berkeley Laboratory, University of California, Berkeley, California, report LBL-26612, 201 pp + appendices.

Montalvo L., F.E., 1991: *Geochemistry of the Chipilapa wells*. CEL, Geothermal Resources Division, El Salvador, internal report (in Spanish).

Montalvo L., F.E., 1994: Appendix to the report: Geochemical evolution of the Ahuachapán geothermal field, El Salvador, C.A. UNU, G.T.P., Iceland, report 10 appendix, 68 pp.

Rogmagnoli, P., Cuéllar, G., Jiménez, M., and Ghessi, G., 1976: Hydrogeological characteristics of the geothermal field of Ahuachapán, El Salvador. *Proceedings of the 2nd United Nations Symposium on the Development and Use of Geothermal Resources*, 1, 571-574.

Steingrímsson, B., Aunzo, Z., Bodvarsson, G.S., Truesdell, A.H., Cuéllar, G., Escobar, C. and Quintanilla, A., 1991: Changes in thermodynamic conditions of the Ahuachapán reservoir due to production and injection. *Geothermics*, 20, 23-38.

Truesdell, A.H., Aunzo, Z., Bodvarsson, G.S., Alonso, J. and Campos, A., 1989: The use of Ahuachapán fluid chemistry to indicate natural state conditions and reservoir processes during exploitation. *Proceedings of the 14th Workshop on Geothermal Reservoir Engineering, Stanford University, USA*, 273-278.